Chalcogenide Letters Vol. 9, No. 5, May 2012, p. 213 - 221

EFFECT OF STARTING MATERIAL SIZE ON STRUCTURAL AND MAGNETIC PROPERTIES OF $(Fe_2O_3)_x$ $(TeO_2)_{1-x}$ GLASS SYSTEM

N.A. ZARIFAH, M. K. HALIMAH*, M. HASHIM, B.Z.AZMI, W.M.DAUD.
Department of Physics, Faculty of Science, University Putra Malaysia, 43400 UPM Serdang, Selangor, Malaysia

Magnetic and structural properties of iron telluride glass whose composition is denoted as $(Fe_2O_3)_x$ $(TeO_2)_{1-x}$ with $(0.1 \leq x \leq 0.3)$ have been explored. Two different series of glass have been prepared using melt quenching technique with different size starting material of iron oxide. The amorphous nature of these glasses was confirmed by the X-ray diffraction spectrum while density of the obtained glasses was measured using Archimedes' principle. Glass stability and glass forming ability was calculated and determined using parameter from DTA curve. It was found that glass stability and glass forming ability of this glass increased as composition iron increased. Magnetic measurement was done at room temperature using vibrating-sample magnetometer (VSM). Results show that these glasses exhibit paramagnetic behavior. Owing to their amorphous structure, these glasses present good soft magnetic properties.

(Received April 20, 2012; Accepted May 22, 2012)

Keywords: iron oxide, paramagnetic, glass system, superparamagnetic

1. Introduction

Telluride glass becomes one of the materials that have been considered in optical devices because of their interesting properties. Telluride glass has physical properties such as high refractive index, low melting temperature, high dielectric constant and high infrared transmission [1]. Because of these features, telluride glass has been considered candidates for optical devices such as optical disk, optical modulators and memory [2].

In recent years, iron based glass has become one of the attracted materials due to their potential applications related to their good soft magnetic properties, such as high saturation magnetization, low core loss and high permeability.

It was reported that glasses containing transition metal ions are used as elements in memory switching devices, cathode material in batteries and gas sensors [3]. Glass with transition metal ions is vital in electronic properties; this is because of the presence of multi-valence states. These glasses also have potential applicability as optical fiber, tunable solid state lasers and efficient laser as well as in the laser spectroscopy due to their thermal and optical properties [4].

The addition of iron oxide in the telluride glass will improve their chemical durability, even when large quantities of other oxides are present. Glasses containing Fe_2O_3 are useful in numerous applications such as in electrochemical, electronic and electro-optic devices [2]. Glass containing iron oxides with high electrical conductivity is useful in applications as sensors in magneto-resistance effect [5]. Several papers have been reported on magnetic properties of glasses in the systems SiO_2-Na_2O-Fe_2O_3 [6], $CaO–P_2O_5–Fe_2O_3$ [7], BaO-Fe_2O_3-TeO_2 [8] and Na_2O-Fe_2O_3-GeO_2 [9].

The purpose of the present paper is to study the effect of size of starting material on the structural and magnetic properties of the Fe_2O_3-TeO_2 glass system in different glass composition as well as the effect of iron oxide in the glass system.

* Corresponding author: halimah@science.upm.edu.my

2. Experimental Section

The binary glass samples $(Fe_2O_3)_x$ $(TeO_2)_{1-x}$ with x = 0.1 to 0.3 with interval of 0.05 were prepared using melt quenching technique. The glasses have been prepared in two different series using two different sizes of starting material of Fe_2O_3.. This glass series is known as FT glass for standard starting material and FTN for nano-sized starting material. Appropriate amounts of Fe_2O_3 and TeO_2 were weighed using electronic balance and mixed in an agate mortar and pestle. The batches were placed in platinum crucible and covered with lid. The batches were preheated in first furnace at 350°C for 30 minutes. The crucible was then transferred to a second furnace and melted at temperature of 950°C for 2 hours. After that, the melt was cast into a preheated cylindrically shaped split stainless steel mould. The sample was later annealed at 350°C for 2 hours. The prepared samples were cut to desired dimension and polished with silicon abrasive papers to obtain smooth and parallel surfaces. The prepared glasses were dark brown in color, free from bubbles and defects. Some of the samples were crushed and grinded to fine powder for further characterization. Amorphous nature of the glass samples was determined using Philips X-Ray Diffractometer (Model PW 1830). The density of the glasses was determined using Archimedes' principle with Acetone (C_3H_6O) as the immersion liquid. Powdered glass was analyzed by UATR-FTIR (Universal Attenuated Total Internal Reflection Fourier Transformation Infrared) spectra recorded using a Perkin Elmer (Spectrum100) FTIR spectrometer in the range of 4000 – 650 cm^{-1}. The thermal properties were performed at 10 °C min^{-1} heating rate with Diamond Pyris DTA (Perkin Elmer). The magnetic properties of samples were measured at room temperature by a vibrating- sample magnetometer (VSM) in a field of 15 kG

3. Results and discussion

In $(Fe_2O_3)x$ $(TeO_2)_{1-x}$ system, TeO_2 is the glass former while Fe_2O_3 acts as glass network modifier. The compositions of the studied glasses are given in Table 1. The structural evolution of glass samples in the function of composition was first checked by determining the amorphous nature of the glass. All the glass samples were found fully amorphous without any peaks present in the XRD results as shown in Figure 1 and Figure 2. X-ray diffraction shows that there are no sharp peaks observed. All the samples were found to be fully in the glass form and presence of a hunch for 2θ around 15°-35°. This indicates that the prepared samples are fully amorphous and have absence of long range atomic arrangement.

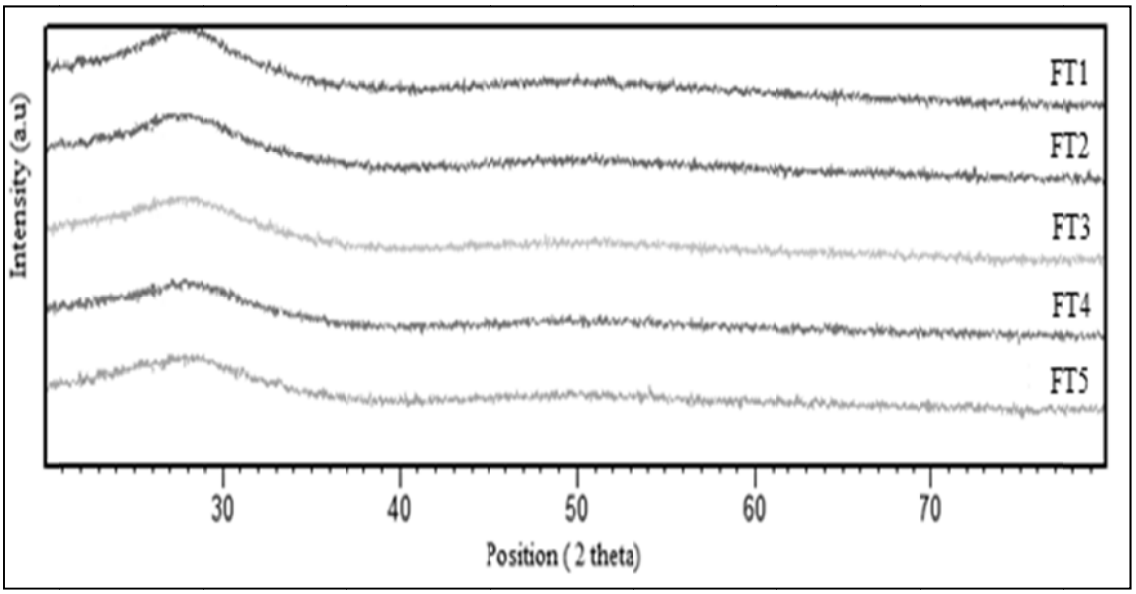

Fig. 1. XRD Spectrum of Fe_2O_3 - TeO_2 (FT) glasses with different composition of Fe_2O_3.

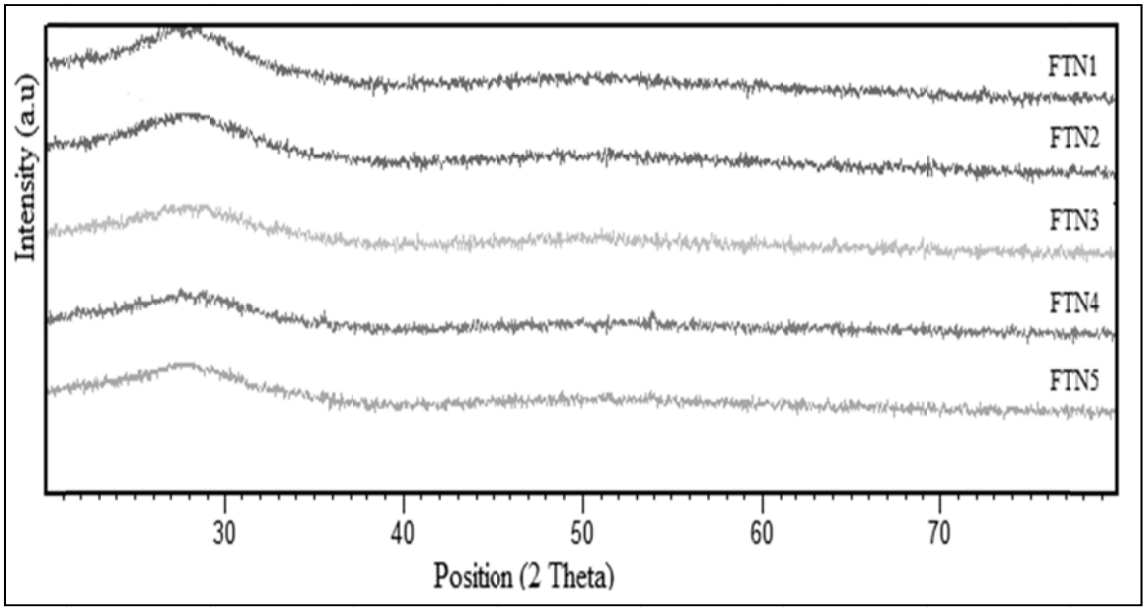

Fig. 2. XRD Spectrum of Fe_2O_3 - TeO_2 using nano material (FTN) glasses with different composition of Fe_2O_3.

Table 1: Abbreviations and composition of $(Fe_2O_3)_x$ $(TeO_2)_{1-x}$ glasses

Sample name	**TeO_2**	**Fe_2O_3 (x)**
FT Series		
FT 1	0.10	0.90
FT 2	0.15	0.85
FT 3	0.20	0.80
FT 4	0.25	0.75
FT 5	0.30	0.70
FTN Series		
FTN 1	0.10	0.90
FTN 2	0.15	0.85
FTN 3	0.20	0.80
FTN 4	0.25	0.75
FTN 5	0.30	0.70

Figure 3 shows the variation of the glass density with the composition of iron oxide. It can be seen that the density decrease with increasing of the iron oxide content. The density of FTN glasses is higher than FT glasses which due to the size of starting material used in FTN glass, where FT glasses has greater volume. It may be assumed that, FT glass series opened glass network structure. The decrease in the density is attributed to the molecular weight of the added iron oxide (55.845 g/mol) which is lower than that of TeO_2 (127.603 g/mol) which will dominate the glass system. The decrease of density may also be due to the change of structure from packed trigonal pyramidal TeO_4 into TeO_3 trigonal pyramid that create open glass network [10].

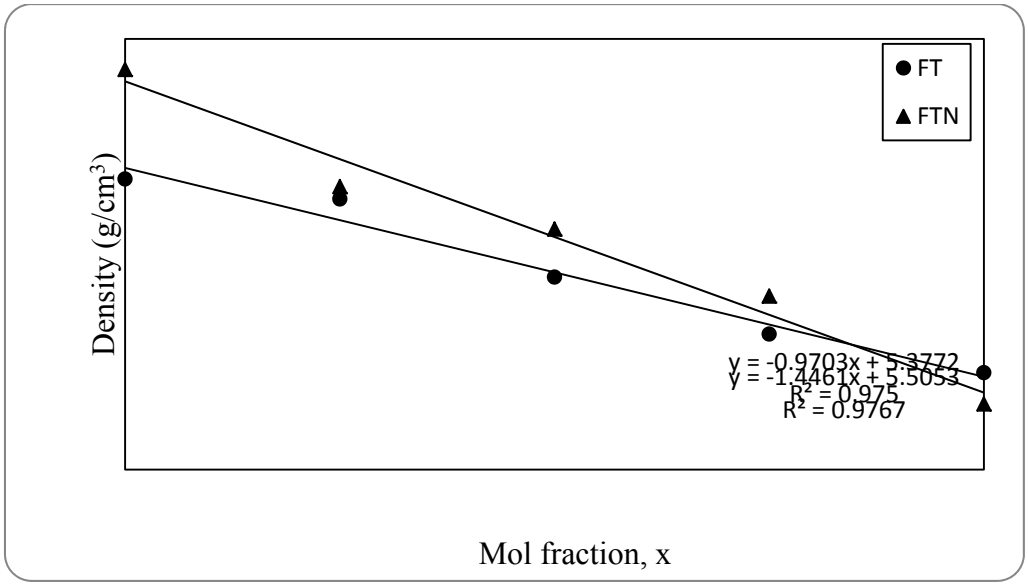

Fig. 3. Variation of the density with composition of Fe_2O_3-TeO_2

IR absorption spectra of the present glasses, FT and FTN glasses are shown in Figure 4 and 5 respectively. Their assigned band positions are reported in Table 2. From these figures, it is shown that there are similar absorption bands for both series, which are ~450, ~660, ~750, ~1240 and ~1750 cm^{-1}. This figure also shows the spectrum of pure TeO_2 and Fe_2O_3. The spectrum of pure TeO_2 is dominated by three bands: ~320, ~670 and ~780 cm^{-1}. By addition of Fe_2O_3 (transition metal) to this sample, the spectrum of these glasses change. The incorporation of Fe_2O_3 into telluride glass enhances the breaking of axial Te–O–Te linkages in the trigonal TeO_4 bipiramyds (tbp). This causes the appearing of TeO_3 (tp) units and the formation of non-bridging oxygens [11].

The absorption band observed at ~450 cm^{-1}, is due to the vibrations of Fe-O bonds that occur in FeO_6 structural units which may be overlapped with the bending mode of Te-O-Te linkages [12] whereas the band at 660 cm^{-1} is due to stretching modes of the trigonal bipyramidal (tbp) TeO_4 structural units with bridging oxygens and also to specific vibrations of Fe-O bonds in FeO_4 units. The intensity of this band increases as an addition Fe_2O_3, ensured the presence of the FeO_4 units in the structure of studied glass [13]. The absorption bands at ~750cm^{-1} has been assigned to trigonal pyramidal (tp) [TeO_3] structural units. In tellurate glasses, the modifier atoms cause the modification of the basic structural units such as TeO_4 trigonal bipyramid and TeO_3 trigonal pyramid with one of the equatorial position occupied by a lone pair of electrons. Introducing of iron into the glass series reinforce the breaking of axial Te-O-Te linkages in the TeO_4 trigonal bipyramids and causes the appearance of TeO_3 (tp) units [11]. The addition of Fe_2O_3 content in the glass system also can accommodate an excess of oxygen through the formation of FeO_6 structural units and the conversion of TeO_4 into TeO_3 structural units. The evolution of the structure can be explained considering the accommodation of the network with excess of oxygen by the conversion of some FeO_4 to FeO_6 structural units.

The weak bands at ~1240 and ~1750 cm^{-1} is owing to the vibrations bands Te-O non bridging bonds of TeO_3 structural units. The increase of Fe_2O_3 in the glass system modifies the vibration intensity of TeO_3 and TeO_4. The existing iron ions in the telluride system may be attributed to the influence of lone pair electron in the glass system. This band also refers to hygroscopic character, which is a characteristic of the –OH bond [12].

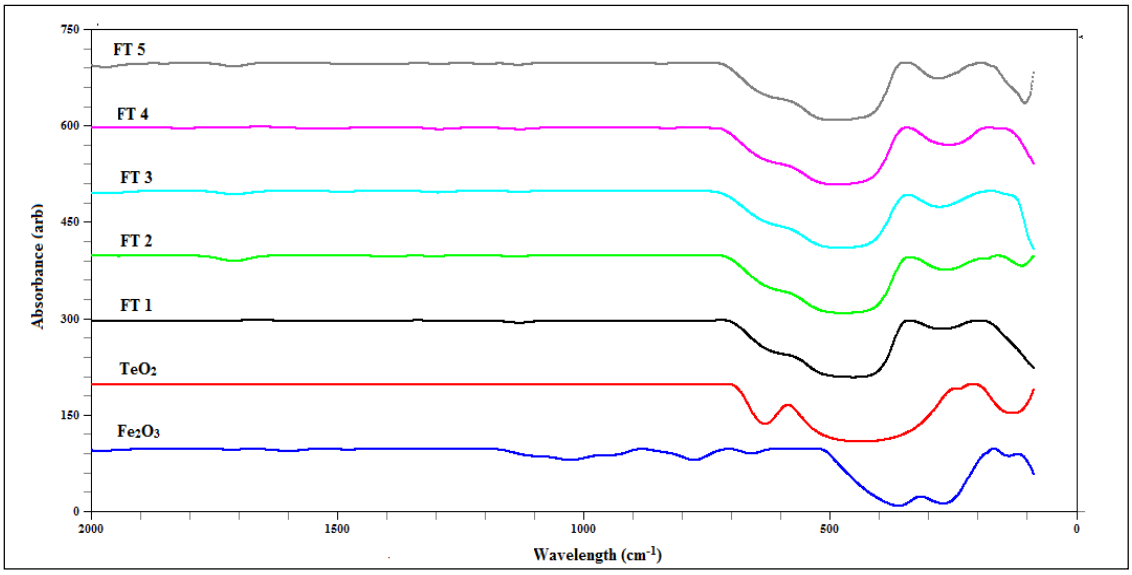

Fig. 4. FTIR Spectra of Fe_2O_3-TeO_2 (FT) Glass system

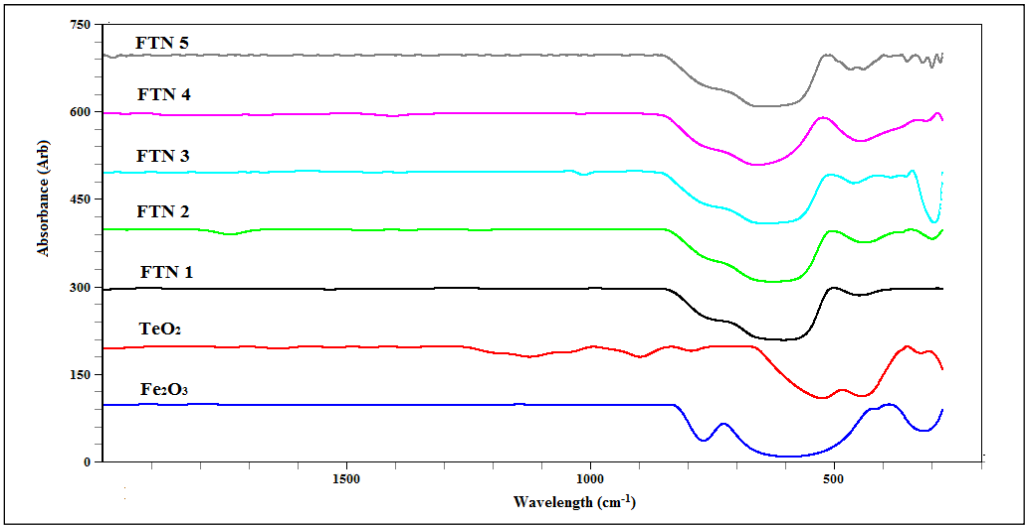

Fig. 5. FTIR Spectra of Fe_2O_3-TeO_2 (FTN) Glass system.

Table 2: Vibration modes of different IR wave numbers

Wave number (cm^{-1})	**Vibration mode**
~450	Specific vibrations of Fe–O bonds in FeO_6 units [12]
~660	Specific vibrations of Fe-O [13] bonds in FeO_4 units [13] Stretching vibration of Te-O in TeO_4 units with bridging oxygen [11]
~750	Stretching vibration of Te-O in TeO_3 units [11]
~1240 and ~1750 cm^{-1}	The vibration bands Te-O non bridging bonds in TeO_3 units [11] Stretching vibration of O-H [12]

Differential Thermal Analysis curves for FT and FTN glass series are shown in Figure 6 and 7 respectively. Four characteristic temperatures, namely the glass transition temperature T_g, the crystallization temperatures T_c, the onset temperature of crystallization T_{oc} and the melting temperature T_m, are determined in all resultant curves and summarized in Table 3. The glass transition temperature T_g represents the strength or rigidity of the glassy structure. T_g values for both FT and FTN glass series increased as Fe_2O_3 increases. The increase of T_g values denote that the glass stability increases, and indicates that Fe_2O_3 has an influence on the increase of glass transition temperature. The T_g value is compared to telluride glass, whereby it is found that the studied glass has higher T_g value than pure telluride glass which is about 610 K, which indicates that the studied glass has high thermal stability as Fe_2O_3 is introduced [14].

Thermal stability, ΔT can be calculated from $T_{oc} - T_g$. In the present study, ΔT is found to increase with the increasing of Fe_2O_3, which indicates an increase in thermal stability. For further confirmation of the above glass stability measurements, thermal stability parameter, S is calculated [15]:

$$S = \frac{\Delta T(T_c - T_{oc})}{T_g} \tag{1}$$

where $(T_c - T_{oc})$ is related to the rate of devitrification transformation of the glassy phase. The obtained value reflects the resistance to devitrification after the formation of glass. Results show that glass with composition of 15% has characteristic of highest thermal stability while S values are inconsistent with others, which may be due to the time of moulding process which will affect the rate of devitrification [15].

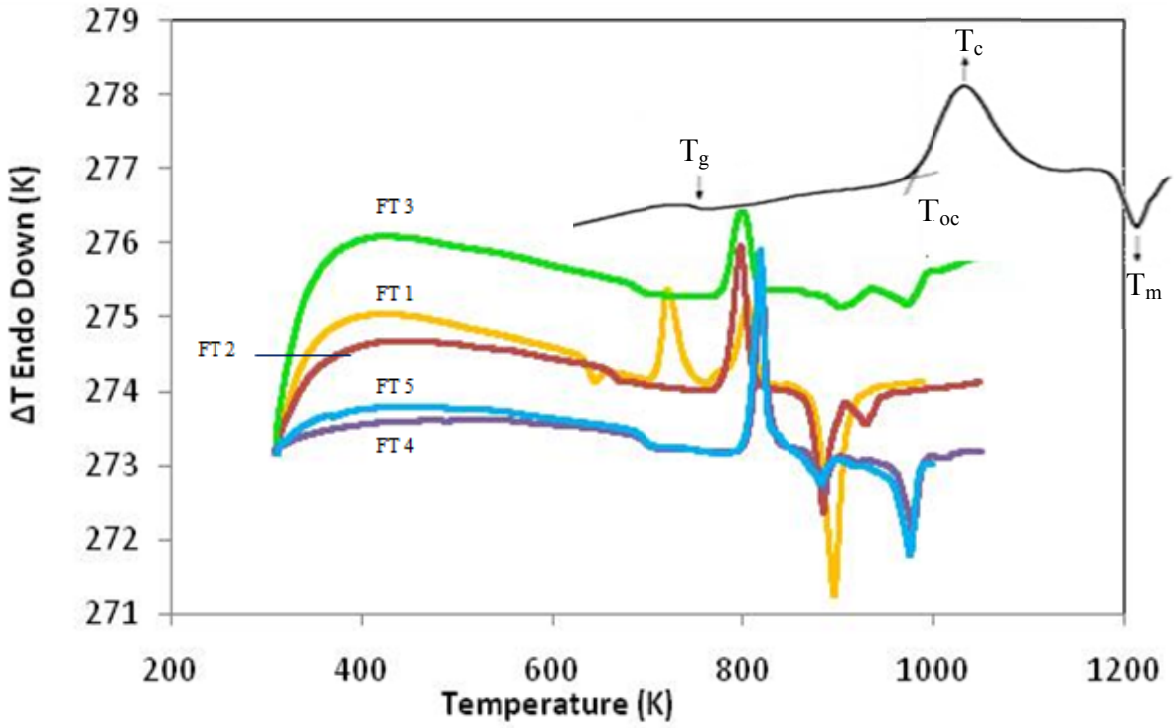

Fig. 6. DTA curve of FT glass system.

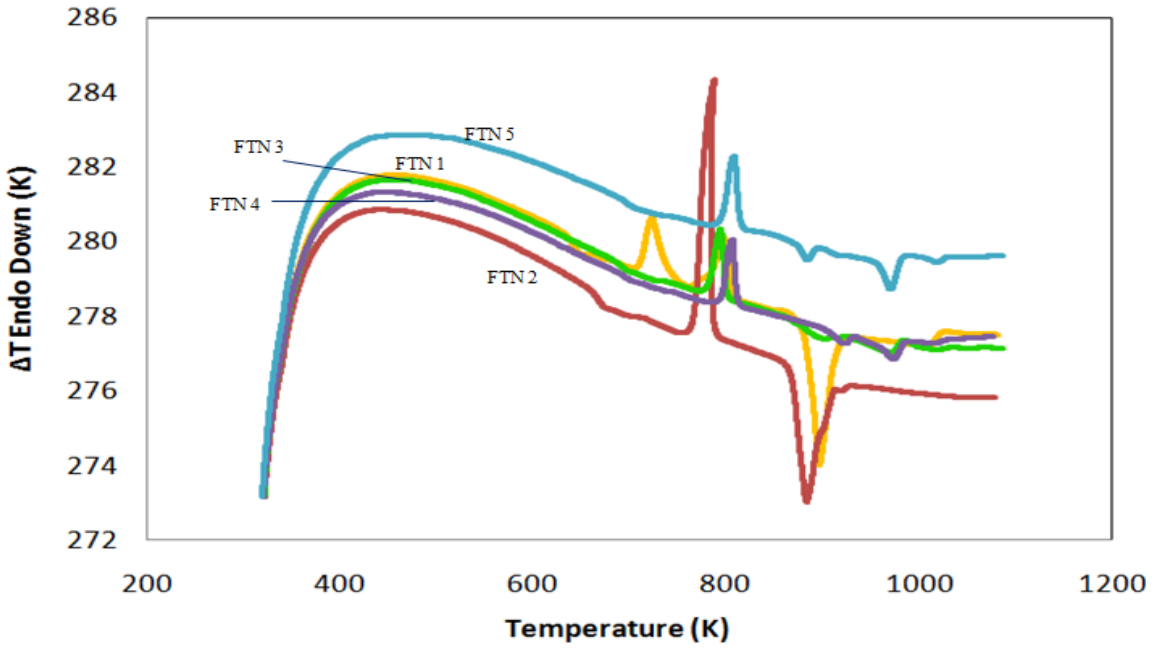

Fig. 7. DTA curve of FTN glass system.

Table 3: DTA parameters for $(Fe_2O_3)_x$ $(TeO_2)_{1-x}$ glass system.

Glass Series	x	Composition	$T_g \pm 0.02$ (K)	$T_{OC1} \pm 0.02$ (K)	$T_{C1} \pm 0.02$ (K)	$T_{C2} \pm 0.02$ (K)	$T_{m1} \pm 0.02$ (K)	$T_{m2} \pm 0.02$ (K)	$\Delta T \pm 0.02$ (K)	$S \pm 0.02$ (K)
FT Glass	0.10	FT 1	638.15	703.15	722.84	804.21	896.12	-	65.00	2.01
	0.15	FT 2	669.15	768.15	797.68	-	886.34	-	99.00	4.37
	0.20	FT 3	688.15	788.15	800.42	-	904.64	974.12	100.00	1.78
	0.25	FT 4	698.15	801.15	818.71	-	886.77	977.51	103.00	2.59
	0.30	FT 5	700.15	805.15	818.26	-	881.69	976.05	105.00	1.97
FTN Glass	0.10	FTN 1	644.70	708.15	722.49	797.08	896.07	-	63.45	1.41
	0.15	FTN 2	668.15	758.15	786.79	-	882.74	-	90.00	3.86
	0.20	FTN 3	689.15	783.15	793.43	-	898.89	975.67	94.00	1.40
	0.25	FTN 4	692.15	794.15	805.40	-	922.39	973.03	102.00	1.66
	0.30	FTN 5	696.15	801.15	807.01	-	883.53	969.85	105.00	0.88

The magnetization (M) as a function of magnetic field (H) of Fe_2O_3 -TeO_2 glass measured by a vibrating sample magnetometer (VSM) at room temperature is presented in Figure 8 and 9. It is observed that all FT glass series and FTN with Fe_2O_3 at 5-25% exhibit paramagnetic behavior while the glass doped with Fe_2O_3 30%, FTN 5 exhibit paramagnetic behavior with contribution of superparamagnetic [16]. The anomaly trend with increasing of Fe_2O_3 in FT glass is explained by the position of magnetic moment in the glass system, which is related with inhomogeneous of Fe_2O_3 in the glass system that probably occurred during preparation process of the glass sample as discussed in the previous study [17]. In FTN glass series, the glass becomes more homogenous as the size of starting material is small. This can be observed by variation of magnetization which increase as composition Fe_2O_3 increases. The insert in Figure 9 is magnification of the FTN 5 glass samples. The magnetic behavior observed is similar to that of soft magnetic materials with

narrow hysteresis loop and low coercivity without saturation point. The quantity of the magnetic phase present in the glass sample is assumed to be small because it cannot be detected by XRD. Thus, magnetic measurements represent a very sensitive means of detecting such transformations which cannot be detected by other physical measurements.

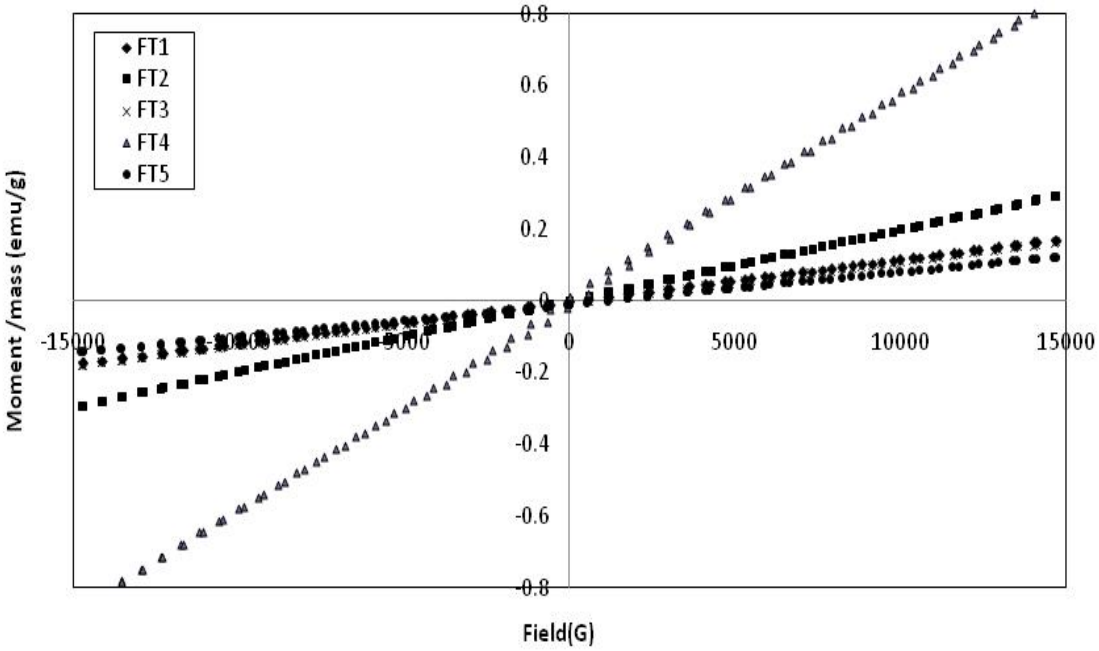

Fig. 8. Magnetic Curve of Fe_2O3-TeO_2 (FT) at varied composition of Iron Oxide.

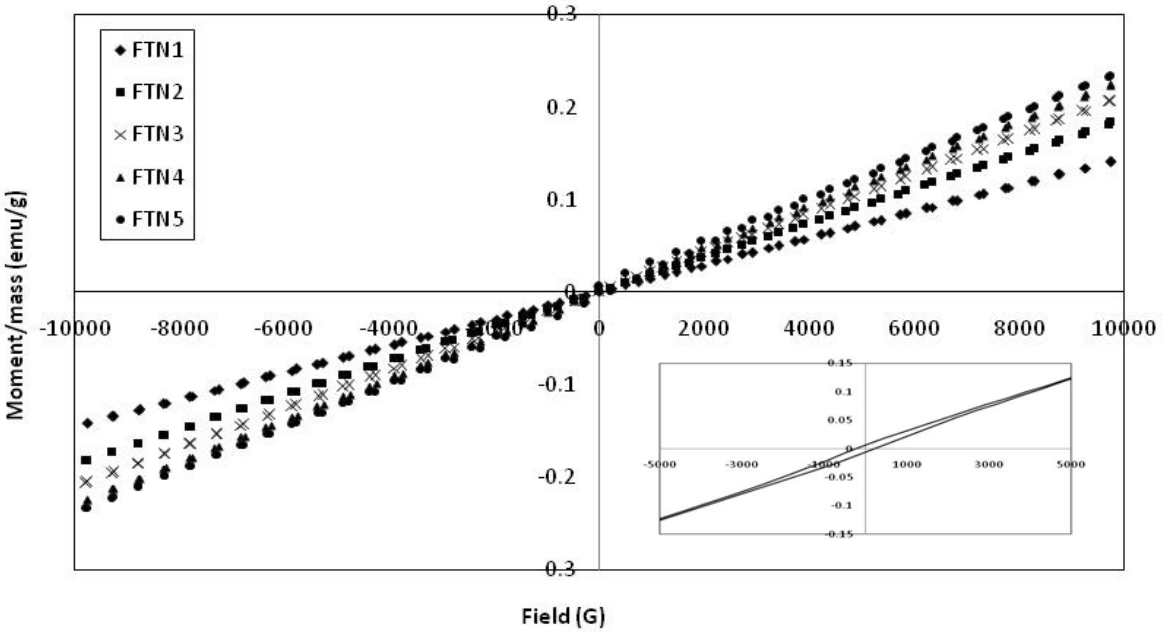

Fig. 9. Magnetic Curve of Fe_2O3-TeO_2 (FT) at varied composition of Iron Oxide

4. Conclusions

Binary iron telluride glass system was synthesized by using two different starting material size of Fe_2O_3. This glass shows improvement in glass stability and glass forming ability with increase of iron oxide. Glass with nano material sized has been found able to improve the soft magnetic properties of Fe_2O_3-TeO_2 and glass iron 30% iron shows paramagnetic with contribution of superparamagnetic behavior.

Acknowledgments

The author would like to thank the Ministry of Science, Technology and Innovation, Malaysia (MOSTI) for the fund under Research University Grant Scheme (RUGS) vote 9199837 and for National Science Foundation (NSF).

References

[1] Tanaka, K., Yoko, T., Yamada, H., and Kamiya, K. Journal of Non-Crystalline Solids, **103,** 250 (1988)
[2] Sabadel, J.C., Armand, P., Cachau-Herreillat, D., Baldeck, P., Doclot, O., Ibanez, A. and Philippot, E. Journal of Solid State Chemistry, **132**, 411 (1997)
[3] Murali, C., Rao, J.L., Narendra, G.L. and Harinathudu, T. Optical Materials, **7**, 41-46. (1997)
[4] Shaltout, I . Journal of Materials Science, **35**, 323– 329. (2000)
[5] Qiu, H.H., Ito, T. and Sakata, H. Materials Chemistry and Physics, **58**: 243-248. (1999) Mekki, A. and Ziq, K.A. Journal of Magnetism and Magnetic Materials, **189,** 207-213. (1998).
[6] Kumar, B. and Christina, H.C. Journal Of Applied Physics, **75,** 6760. (1994)
[7] Laville, H., Barnier, J.C. and Sanchez, J.P. Solid State Communications, **27,** 259 (1978)
[8] Mekki, A., Holland, D., Ziq , K.A. and McConville, C.F. Journal of Non-Crystalline Solids, **272**, 179-190. (2000)
[9] Shankar, M.V. and Varma, K.B.R. Journal of Non-Crystalline Solids, **243**, 192-203. (1999)
[10] Rada, S., Dan, V., Rada, M. and Culea, E. Journal of Non-Crystalline Solids, **356**, 474–479. (2010)
[11] Ardelean, I. and Păşcuţă, P. Materials Letters, **58**, 3499 (2004)
[12] Timar, V., Lucăcel – Ciceo, R. and Ardelean, I. Semiconductor Physics, Quantum Electronics & Optoelectronics, **11,** 221-225. (2008)
[13] Mallawany R.E. Journal of Material Research, **18**, 2 (2003)
[14] Lafi, O. A.and Imran, M.M.A. Journal of Alloys and Compounds, **509,** 5090 (2011)
[15] Maximina Romero-Perez, Jesús Ma. Rincón, Carlos J.R. González Oliver , Claudio D'Ovidio, Daniel Esparza, Materials Research Bulletin, **36**, 1513 (2011).
[16] Zarifah, N.A, Halimah, M. K. Hashim, M., Azmi, B. Z. and Daud, W. M. Chalcogenide Letters. **7**(9), 565 (2010)